biophysica

MDPI

Article

Exploring Chemokine Homodimer Stability: Structural Insights into CXC and CC Interfaces

David Budean [1], Yasser Almeida-Hernández [2], Jitendra Pandey [1], Joel Mieres Pérez [2], Elsa Sánchez García [2] and Ellinor Haglund [1,*]

[1] Department of Chemistry, University of Hawaii at Manoa, Honolulu, HI 96822, USA; dbudean@hawaii.edu (D.B.); jitendra@hawaii.edu (J.P.)
[2] Fakultät für Bio- und Chemieingenieurwesen, Technische Universität Dortmund, Emil-Figge Str. 66, 44227 Dortmund, Germany; yasser.almeida@tu-dortmund.de (Y.A.-H.); joel.mieresperez@tu-dortmund.de (J.M.P.)
* Correspondence: ellinorh@hawaii.edu; Tel.: +1-(808)-956-5163

Abstract: Chemokine ligands play a pivotal role in immune response by mediating cell migration and coordinating cellular processes through interactions with chemokine receptors. Understanding their sequence and structural integrity is crucial for elucidating their biological functions and potential therapeutic applications. In this study, we investigate the dimer interface between two distinct homodimer topologies: CXC and CC homodimers. Despite nearly identical monomeric structures, the rigid CXC interface is characterized by interactions between the N-loop/β-sheet regions, while the more flexible CC interface involves interactions through the unstructured N-terminal regions. Our structural and biophysical analyses indicate no significant differences in the free energy of folding (2–8 kcal/mol) and binding (10–14 kcal/mol) between the two homodimer topologies, showing that their free energy is primarily driven by sequence. We hypothesize that the biological signal is driven by the malleability of the dimer, depending on the binding interface. Understanding these structural dynamics opens new possibilities for designing chemokine-based therapeutics to modulate immune responses in diseases such as cancer, inflammation, and autoimmune disorders.

Keywords: chemokines; homodimer; dimer interface; protein–protein interaction; conformational dynamics; protein folding

Citation: Budean, D.; Almeida-Hernández, Y.; Pandey, J.; Pérez, J.M.; Sánchez García, E.; Haglund, E. Exploring Chemokine Homodimer Stability: Structural Insights into CXC and CC Interfaces. *Biophysica* **2024**, *4*, 561–572. https://doi.org/10.3390/biophysica4040037

Academic Editor: Attila Borics

Received: 1 November 2024
Revised: 22 November 2024
Accepted: 24 November 2024
Published: 27 November 2024

1. Introduction

Chemokine ligands are essential signaling molecules that orchestrate the movement and activation of immune cells, thereby shaping the immune response to infection, injury, and inflammation. These small proteins function by binding to specific chemokine G protein-coupled receptors (GPCRs) on the surface of immune cells, a process that triggers a cascade of intracellular signaling events leading to cell migration and activation [1]. The specificity of this interaction is mainly determined by the structural characteristics of the chemokine ligands and their receptors [2]. Little is known about the formation of homodimers among chemokines crucial for receptor activation and function, which are critical for their full biological activity [3,4]. Homodimerization enhances the binding affinity of these chemokines to their receptors, amplifies signal transduction, and ensures more efficient and sustained immune responses [5]. Understanding the role of chemokine ligands and their dimerization is fundamental for unraveling the complexities of immune regulation and for developing therapeutic strategies aimed at modulating immune responses in various diseases.

While chemokine receptors can be activated by various oligomeric states of the ligand, including monomers, homodimers, and heterodimers [6], it is proposed that homodimers particularly enhance receptor activation, leading to an amplified inflammatory response [3,4]. Furthermore, the X residue inserted between the two cysteines of CXC

proteins aids in orienting its N-terminus to the pocket of the receptors for optimal binding [7]. Thus, the CXC/CC motif directly influences receptor-binding specificity within each CXC/CC subfamily. Despite the low sequence identity, the monomeric proteins exhibit nearly identical native states, yet the binding interfaces between the two subfamilies differ significantly (Figure 1). The CXC dimers are formed through interactions between the β-strands of each monomer, supported by the α-helix, whereas CC dimers have an unstructured N-terminal domain that forms the binding interface (Figure 1A,B). The CC configuration orients β-strand 1 and the α-helix away from the interface. The construction of the homodimer interface, β-strand 1 versus the unstructured N-terminus, also contributes to the malleability of the dimer. The more rigid CXC dimers ensures stable interactions with the receptor affecting the specificity, such as tight binding to glycosaminoglycans (GAGs) and precise receptor activation [8,9], fine-tuning the biological response. This specificity may lead to a narrower range of functional interactions, such as directing neutrophil recruitment and mediating responses to infection and injury [10,11]. In contrast, the flexible interface of CC dimers may contribute to functional diversity, enabling these chemokines to interact with multiple receptor types as seen in the activation of CC receptors, where CC dimers often exhibit broader receptor-binding specificity, i.e., interacting with multiple receptors [3,12–14].

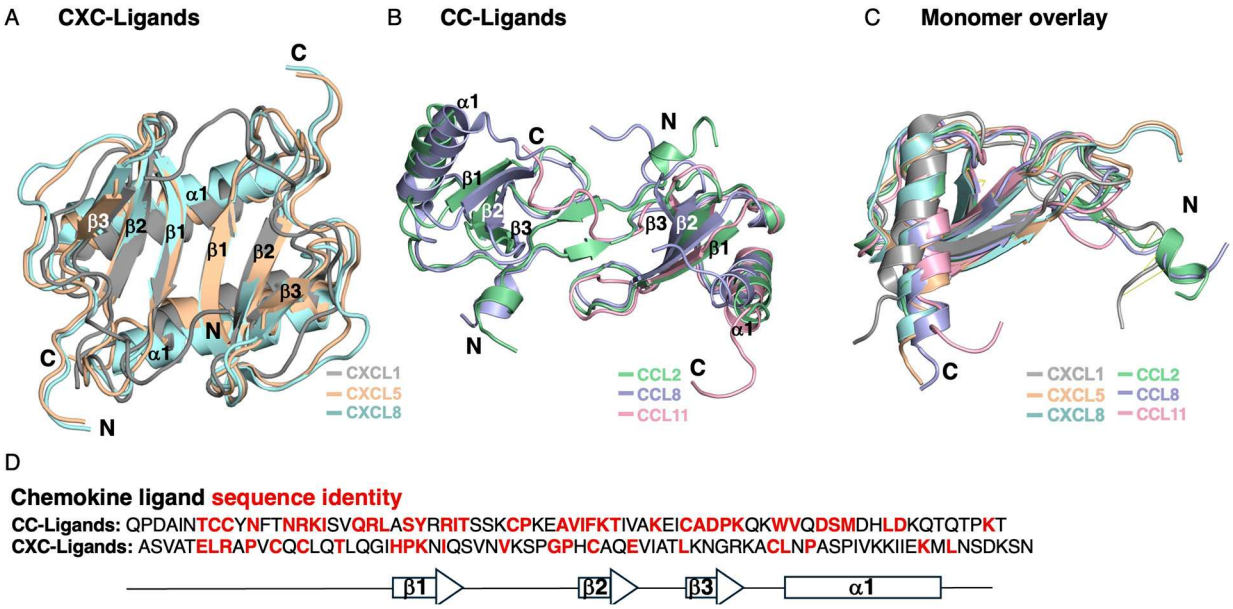

Figure 1. Structural overlay of chemokine ligands. Despite the low sequence identity, the CXC ligands share structural homology with an RMSD (root-mean-square deviation) score of 2.31 and 2.98 for CXCL1–CXCL8 and CXCL1–CXCL5 [15] and 1.54 and 3.10 for CCL2–CCL8 and CCL2–CCL11 using the pairwise Structure Alignment from the PDB (jFATCAT-rigid) [16]. (**A**) CXC ligands (PDB ID: 1MGS, 2MGS, and 1IL8). (**B**) CC ligands (PDB ID: 1DOK, 7S5A, and 1EOT). (**C**) CXC and CC monomer overlay. (**D**) Sequence alignment for CXC and CC ligands.

In this study, we examine the biophysical properties of homodimers from the CXC and CC family. Specifically, our research focuses on six chemokine ligands: CXCL1, CXCL5, CXCL8, CCL2, CCL8, and CCL11. By examining two distinct homodimer topologies—CXC and CC—we uncover critical differences in the dimers despite their nearly identical monomeric forms. Through a combination of structural and biophysical analyses, we demonstrate that both interfaces have similar binding energies ranging between 6 and 9 kcal/mol. The two most stable dimers are formed for CXCL8 and CCL2 due to the robust network of hydrogen bonds, hydrophobic interactions, and salt bridges. These insights not only deepen our understanding of chemokine dimerization but also pave the way for

developing chemokine-based therapeutics to modulate immune responses in diseases such as cancer, inflammation, and autoimmune disorders.

2. Materials and Methods

Cloning, expression, and purification. The CXC and CC proteins target genes were designed as described [15] and cloned into a pET-32a Xa/LIC vector (GenScript, NJ, USA). All proteins were recombinantly expressed as a fusion protein from the pET-32a Xa/LIC vector, expressed in *E. coli* BL(21)DE3 cells (Agilent, CA, USA) and purified as described [15]. Purity was evaluated by SDS-PAGE; the identity of CXC proteins was previously published [15], while CC protein identities were confirmed through mass spectrometry (Figure S1).

Thermodynamic experiments. Equilibrium titration and thermal-melt studies were performed using a Chirascan v100 spectrometer (Applied Photophysics, Leatherhead, UK). Circular dichroism (CD) spectra were collected in the far UV range, 260–190 nm, at a protein concentration of 30 μM (to ensure dimeric proteins [15]) in a 1 mm cuvette to assess secondary-structure formation. Equilibrium titration was conducted by monitoring the fraction of denatured protein via CD at 222–216 nm in the presence of 0–8 M guanidinium hydrochloride (GdmCl), using a 10 mM potassium phosphate buffer at pH 7.4 and 25 °C. The change in Gibbs free energy (ΔG) was calculated using the following equation:

$$\Delta G_{D-N} = -RTlnK = -2.3RTlogK \quad (1)$$

where the equilibrium constant (K) is the ratio between the denatured state [D] and the native state [N], R is the gas constant, and T is the temperature in Kelvin.

The fraction of the observed species (F_{app}) is represented by a two-state fit [17] shown by

$$F_{app} = \frac{Y_N - Y}{Y_N - Y_D} \quad (2)$$

where the Y is the CD signal for the specified species, the two fractions [D] and [N]. The observed CD signal is plotted against denaturant concentration. The fitting equation for a two-state model is as follows:

$$Y = Y_N f_N + Y_D f_D \quad (3)$$

Thermal-melt experiments. Thermal denaturation was performed by increasing the temperature from 25 °C to 90 °C at a rate of 1 degree per minute, with data collected at 1 °C intervals. The CD signal was recorded at 230–215 nm. The temperature was controlled by the built-in Peltier device, ensuring stable thermal conditions during the experiment. The protein samples were prepared in 10 mM potassium phosphate buffer, pH 7.4, at a concentration of 30 μM. The fraction of unfolded protein was calculated from the CD data using the following equation:

$$f_D = \frac{CD(T) - CD_N}{CD_D - CD_N} \quad (4)$$

where $CD(T)$ is the CD signal at a given temperature, CD_N is the signal for the fully native protein, and CD_D is the signal for the fully denatured protein. The thermal denaturation curves were fitted to a two-state model to determine the melting temperature (Tm), the temperature at which 50% of the protein is unfolded. The data were analyzed using Global 3.1.0.78 Thermodynamic Analysis software (Applied Photophysics, Leatherhead, UK), which allows for the fitting of a nonlinear regression to the denaturation curve. The results were further processed using Kaleidagraph to plot the fraction of unfolded protein as a function of temperature.

Due to the slow dissociation rates of CXC dimers [15] compared to CCL11 dimers [18], CXC protein was not able to equilibrate within the 1 min settling time. Instead, a stepwise heating method was used for CXC chemokines where measurements were collected at 2 °C intervals with a 5 min settling time. Furthermore, aggregation was observed at higher temperatures with the long settling times (Figure S2).

CCL11 dimer prediction. The structure of the CCL11 homodimer was predicted with a local implementation of AlphaFold2-Multimer (version 2.3.2) (Figure S3) [19]. The sequence of residues 24–97 was used for the prediction, where 5 models were obtained, using 5 seeds per model. The models were ranked with the combined score of ipTM + pTM, and the best one was chosen for further analysis.

Homodimer-binding affinity estimation. The following structures were used for the predictions: CCL2 [20], CCL8 [21], CXCL1 [22], CXCL5 [23], and CXCL8 [24]. For CCL11, we used the AlphaFold model explained before. PPI-Affinity [25] was employed to predict the binding affinity of the homodimers, using the protein–protein trained model. PPI-Affinity is a structure-based machine learning method that analyses the residues in the binding interface for free-energy estimations.

3. Results and Discussion

Structural analysis. The monomeric overlay (Figure 1C) suggests that the proteins likely maintain similar structural integrity, which would result in closely aligned far-UV CD spectra for chemokine ligands. However, visual inspection of core residues and the binding interface combined with CD (Figure 2A) experiments reveals that the diversity within each family is as extensive as that between the CXC and CC families. The different binding interfaces may lead to conformational changes, such as shifts in α-helix or β-strand orientation, resulting in slight variations in ellipticity values or minor peak shifts observed between the dimers (Figure 2). The CD spectra of CXC dimers show two minima, one at 222 nm and one at 208 nm, characteristic of α-helices and β-strands, respectively. The helix of CXCL8 is four amino acids longer than the helices of CXCL1 and CXCL5, explaining its more pronounced minimum at 222 nm (Figure 2A). CXCL5 displays a shifted peak in height relative to CXCL8, with the lowest minimum at 208 nm. CXCL1 shows the largest shifts, with a minimum above 200 nm and a plateau at 222 nm. The CD spectra of CC dimers show only minor shifts of the single minimum at 208 nm, as expected from the structural overlay (Figure 2B). This is in agreement with previously published CD spectra of CCL11 [18]. The CD spectra of CC dimers depict a more β-sheet-like structure compared to CXC dimers (Figure 2). In CXC dimers, the dimer interface stabilizes both the helix and a β-strand region, with the helix becoming somewhat extended upon dimerization [26], which leads to a more defined minima at 222 nm.

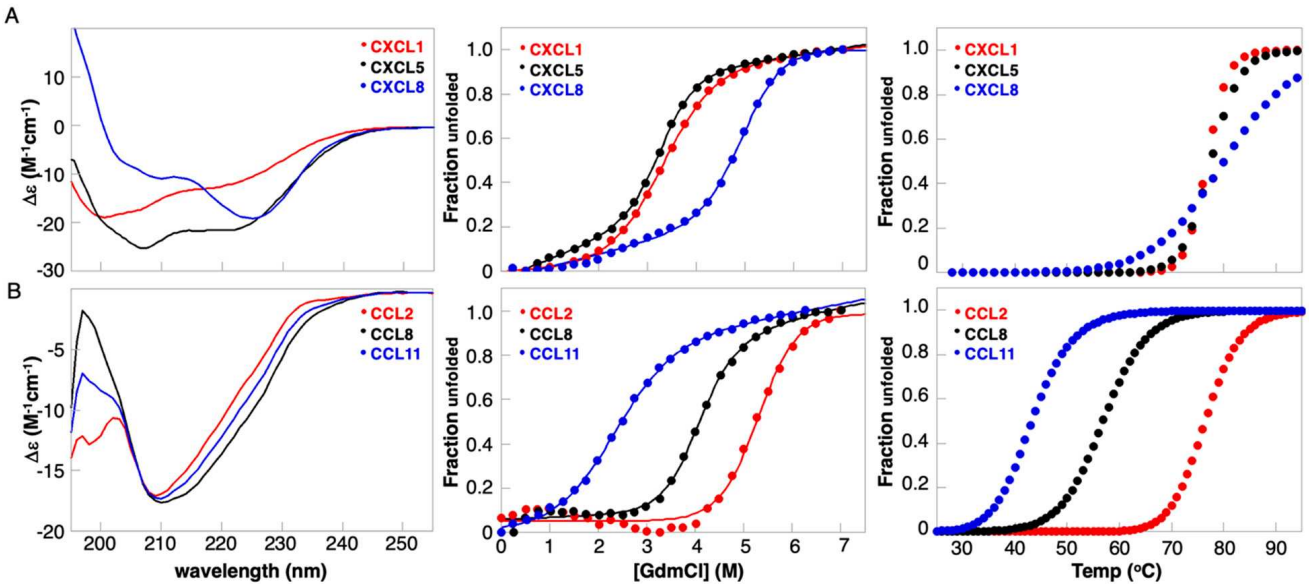

Figure 2. Biophysical characterization. (**A**) CXC ligands and (**B**) CC ligands depicting CD spectra and thermodynamic experiment utilizing temperature and chemical denaturant.

Thermodynamic experiments. The Tm is calculated from thermal equilibrium titrations between 25 and 90 °C for CXC and CC dimers (Figures 2 and S2). The CXC chemokines have a higher Tm than CC proteins, which suggest higher thermal stability as a family. Interestingly, CXCL8 demonstrates incomplete unfolding even at 90 °C, which has been previously observed for CXCL7 [27]. The change in the slope of CXCL8 (Figure 2B) is attributed to this incomplete unfolding event. The Tm^2 for CXCL1 and CXCL5 are within one degree Celsius, supporting the trend observed with the chemical denaturant. The data show bimodal behaviors for all ligands except CCL8 (Table 1). The data for CCL8 were fitted to a single transition, with a Tm^2 of 56.9 ± 0.2 °C. This agrees with the equilibrium data from the chemical denaturant, showing a pronounced bimodal behavior at low GdmCl for all proteins except CCL8 (Figure 2B). This indicates that we can only obtain $2D \rightarrow N_{Dimer}$ for CCL8, while the ground states $2D \rightarrow 2N_{Monomer} \rightarrow N_{Dimer}$ can be obtained for all other proteins. For CCL11, the thermal melt reveals two distinct transitions occurring at the same temperature, suggesting a three-state behavior. This is in agreement with previously published kinetic data for CCL11 showing two transitions at the same GdmCl concentration [18]; i.e., the unfolding transition is occurring simultaneously with the dissociation of the dimer [28].

Table 1. Calculations of thermal stability (Tm) in 10 mM phosphate buffer at pH 7.4.

	Tm^1 °C	**Tm^2 °C**
CXCL1 [a]	53.9 ± 0.6	76.8 ± 0.1
CXCL5 [a]	56.6 ± 0.3	77.6 ± 0.1
CXCL8 [a]	41.9 ± 0.3	80.0 ± 0.3
CCL2 [b]	64.8 ± 0.4	75.9 ± 0.1
CCL8 [c]	n.d.	56.9 ± 0.2
CCL11 [b]	41.0 ± 0.6	40.6 ± 2.3

[a] Data fitted to no baseline. [b] Data fitted to a single baseline. [c] Data fitted to a double-baseline model. Tm^1 is the fit of the minor transition observed at a lower temperature while Tm^2 is the fit for the major transition observed at a higher temperature.

Given the variability in bimodal behavior, we applied a two-state model to fit all equilibrium titrations (Figure 2B), allowing us to analyze the $2D \rightarrow N_{Dimer}$ transition. As discussed in detail previously [15], CXCL1 shows two-state behavior, whereas CXCL5 and CXCL8, which display a more pronounced bimodal trend at lower denaturant concentrations, may fit better to a three-state model [28]. Concentration-dependent studies combined with kinetics experiments revealed that all CXC dimers fold through an on-pathway monomeric intermediate ($N_{Monomer}$) state, $2D \rightarrow 2N_{Monomer} \rightarrow N_{Dimer}$ [15,18]. Our data show that CXCL8 and CCL2 are the most stable proteins, with a ΔG for folding of 7.07 ± 0.10 kcal/mol and 7.91 ± 0.10 kcal/mol, respectively (Table 2). The least stable proteins are CXCL1 and CCL11 with a ΔG of 3.68 ± 0.03 kcal/mol and 2.50 ± 0.08 kcal/mol, respectively. Taken together, the results from thermal and chemical unfolding experiments are consistent, showing a major transition at elevated temperatures and higher denaturant concentrations (Figure 2). This suggests that the unfolding event occurs in a major phase while the minor phase is likely the dissociation between the dimer and monomer. However, analyzing the phases is challenging due to both the small structural changes involved in dimer dissociation, and the conditions that promote dissociation may also induce protein unfolding. This was observed in CCL11, where the two melting transitions nearly coincide. This overlap complicates the interpretation of CD data, making it difficult to distinguish between dissociation and unfolding transitions.

Table 2. Equilibrium titrations in 10 mM phosphate buffer at pH 7.4 at 25 °C.

	MP **M**	$\mathbf{m_{D\text{-}N}}$ $\mathbf{M^{-1}}$	**ΔG** **kcal/mol**
CXCL1 [a]	3.31	0.82	−3.68 ± 0.03
CXCL5 [b]	3.32	1.23	−5.57 ± 0.04
CXCL8 [b]	5.00	1.04	−7.07 ± 0.10
CCL2 [a]	5.29	1.10	−7.91 ± 0.10
CCL8 [a]	4.17	0.93	−5.27 ± 0.06
CCL11 [b]	2.33	0.79	−2.50 ± 0.08

[a] Data fitted to a two-state equation with a straight baseline. [b] Data fitted to a two-state equation with a sloped baseline.

To obtain information regarding the binding free energies of the dimers (Table 3), we employed the PPI-Affinity method [25]. This method uses a support-vector machine-based model trained with molecular descriptors of the residues in the interfaces of protein complexes to compute the binding free energy. PPI-Affinity was not trained to predict the unfolding free energy, and it shows a mean absolute error (MAE) = 1.8 kcal/mol for the protein–protein trained model. Our results show no significant difference between the two chemokine homodimeric topologies, i.e., 14.3 kcal/mol and 12.6 kcal/mol for CXCL8 and CCL2, respectively. Interestingly, the equilibrium data of CXCL8 and CCL2 show the most pronounced bimodal behavior. The PPI-Affinity calculations include the effect of the solvent implicitly. The model was trained using experimental data that was done in solution. Nonetheless, the trends observed in the calculated free energies agree with the number of residues and contact types within the binding interface, where CXCL8 and CCL2 have the strongest binding interface with four contacts including salt-bridges (Figure 3 and Table 4). Based on our in silico and in vitro results, we hypothesize that the rigid versus flexible binding interface may not contribute to the stability of the dimers. Visual inspection of the binding interface further supports the trends of estimated binding energies within each family (Figure 3). The interface is built from a network of hydrogen bonding with additional side-chain contacts to stabilize the interaction. For the CXC homodimers, CXCL8 has two non-polar contacts and two salt bridges; CXCL5 has two polar and two non-polar contacts; and CXCL1 has one polar and two non-polar contacts. For the CC homodimers, CCL8 has two polar contacts and one non-polar contact; CCL2 has two polar contacts; and CCL11 has two non-polar contacts. A further visual inspection of the hydrophobic core supports the thermodynamic analysis (Figure 3). Among the proteins, CCL2 is the most stable with 12 hydrophobic contacts, followed by CXCL8 with 11, CCL8 with 10, CXCL1 with nine, CXCL5 with 8, and CCL11 with six, the last of which is the least stable (Figure 3). The hydrophobic core is further stabilized by aromatic residues and hydrogen bonding patterns between secondary structures. Specifically, CCL2 is stabilized by F43 and W59, with four hydrogen bonds between β-strands 2 and 3 (V41-A53 and F43-I51). CXCL8's stability is reinforced by F17 and one hydrogen bond between β-strands 2 and 3 (I34-L51). CCL8 is stabilized by F43, W59, and six hydrogen bonds between β-strands 2 and 3 (I31-A40, V41-A53, and F43-V51). In contrast, CXCL5 lacks additional aromatic residues or hydrogen bonds in the core, while CXCL1 has one stabilizing hydrogen bond between β-strands 2 and 3 (V40-L52), making it moderately more stable than CXCL5. Finally, CCL11 is supported by F41, W57, and four hydrogen bonds between β-strands 2 and 3 (V39-A51 and F41-I49).

Table 3. Binding free energies estimated with PPI-Affinity.

	Score kcal/mol
CXCL1(GROα)	−9.7
CXCL5 (ENA78)	−10.4
CXCL8 (IL-8)	−14.3
CCL2 (MCP-1)	−12.6
CCL8 (MCP-2)	−11.6
CCL11 [a] (Eotaxin)	−10.9

[a] The data are obtained from an AlphaFold prediction of the CCL11 homodimer.

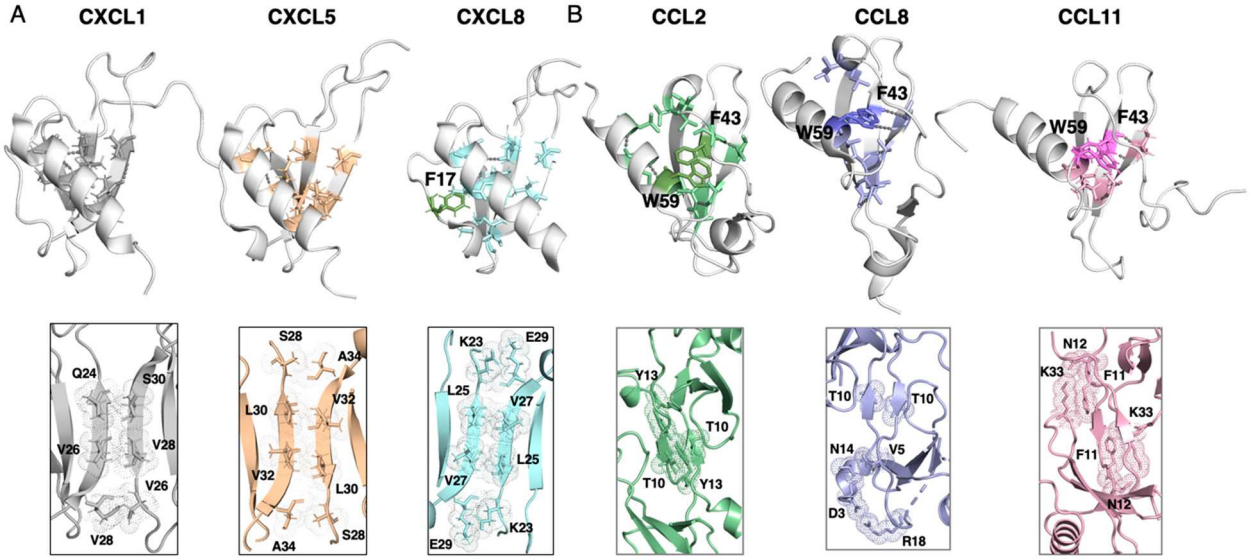

Figure 3. Residue analysis of CXC and CC proteins. (**A**) depicts CXC ligands while (**B**) depicts CC ligands. Top: The core residues are shown as sticks, where the hydrophobic core is shown in light colors. The aromatic residues are shown as in darker colors, and the hydrogen bonds are shown as grey dashed lines. Bottom: The dimer interface is shown as sticks, depicting the residue numbers and residue types. The backbone hydrogen bonds are excluded to emphasize the core interactions.

Table 4. Visual inspection of CXC and CC ligands.

	Hydrophobic Core	Hydrogen Bonding	Aromatic Core	Dimer Interface
CXCL1	9	V40-L5	-	Q24-S30, V26-V28, V28-V26
CXCL5	8	-	-	S28-A34, L30-V32, V32-L30, A34-S28
CXCL8	11	I34-L51	F17	K23-E29, L25-V27, V27-L25, E29-K23
CCL2	12	V41-A53, F43-I51	F43, W59	T10-T10, Y13-Y13
CCL8	10	I31-A40, V41-A53, F43-V51	F43, W5	T10-T10, N14-V5, D3-R18
CCL11	6	V39-A51, F41-I49	F41, W57	N12-K33-F11, K33-F11-N12

Our analysis highlights the complex relationship between chemokine sequence diversity, structural stability, and dimer formation. Despite similar monomeric structures, chemokine ligands exhibit unique CD spectral profiles, particularly for the rigid CXC homodimers, and thermal behavior, suggesting that sequence-specific interactions drive stability and binding-interface characteristics. The thermal melts confirm that the notable stability differences across chemokines are linked to variations in hydrophobic core contacts and hydrogen bonding rather than the dimer interface. These findings underscore the role of hydrophobic interactions and aromatic residues in stabilizing dimeric chemokine structures, ultimately determining their biophysical and functional diversity. The stability ranking, led by CCL2 and CXCL8, provides insights into how chemokine sequence

variations influence folding energetics, with implications for understanding chemokine behavior under physiological conditions.

Intriguing insight. CCL11 has one of the lowest binding free energies with the lowest free energy for folding, both from thermal and chemical stability. The observation from thermal denaturation of the overlapping free energies gives rise to a two-state transition, although the mechanism is $2D \rightarrow 2N_{Monomer} \rightarrow N_{Dimer}$. Remarkably, the monomeric protein is isolatable at acidic pH [29], where the dimer interface is broken without unfolding the structure. This pH most likely affects the lysine residue 33 (K33) by altering its hydrogen bonding and electrostatic interactions. Our experiments were conducted at pH 7.4, where the lysine would still carry a positive charge (since its side-chain pKa is around 10.5). However, the more neutral environment could reduce competition from free H^+ ions, potentially stabilizing any electrostatic interactions of the dimer interface, leading to a more stable dimer.

Potential role of ligand homodimer in receptor binding. In this work, we studied CXC and CC proteins with in vitro biophysical characterization utilizing CD measurements and binding-free-energy estimations. Understanding the role of protein dimers, their binding interface, and binding affinity is crucial in understanding allosteric effects and receptor activation.

A sequence alignment of the six sequences reveals that the four cysteine residues and a proline (P55 in CCL8) in loop III are fully conserved (Figure S4), which is crucial for the stability and structural integrity of chemokines. The conserved proline in loop III, along with the unstructured N-terminal region, is thought to be important for receptor recognition [12,30]. In contrast, the core residues show only partial conservation (Figure 3), with four conserved residues (L25, V41, V60, and tryptophan) present in all proteins except CXCL1 and CXCL5, contributing to the stabilization of the core (Figure S4). Our structural and biophysical analyses indicate that sequence diversity governs both protein stability and half-life as well as dimer association. The CXC proteins form an interface between β-strand 1 of each monomer in the opposite orientation forming a rigid dimer, while the dimer formation of CC proteins depends on contacts between the flexible N-terminal forming a symmetric dimer. This diversity may play a critical role in allosteric effects and receptor activation.

Chemokine receptors represent one of the largest drug target families, making receptor activation a well-researched area. Consequently, the mechanisms governing receptor function are relatively well understood [31]. However, less is known about how these receptors interact with the various oligomeric forms of their chemokine ligands. Homodimers are formed through non-covalent interactions between two identical ligands, creating two receptor-binding sites. This structural feature allows a homodimer to simultaneously engage with two receptors, either on the same cell or on neighboring cells, influencing the binding affinity and signaling dynamics [4,12,32,33]. The effects of homodimer binding to GPCRs may include the following: (i) dual-receptor activation on the same cell, which could amplify or modulate downstream signaling pathways—this simultaneous engagement of two receptors may lead to stronger or more sustained signaling compared to monomeric ligand binding [3,30]—and (ii) receptor cross-linking, which may influence signaling outcomes such as increased receptor internalization, prolonged signal duration, or biased signaling toward specific pathways [34]. If the homodimer binds to receptors on separate cells, those cells must be close enough for the homodimer to span the distance between the receptors. In such scenarios, the homodimer can activate signaling pathways in both cells simultaneously, potentially promoting coordinated cellular responses. Homodimer activity may also depend on allostery [5,35]; when one monomeric pair bind to the receptor, the second monomer can either remain active from positive allostery [36] or be rendered inactive from negative allostery [37]. Furthermore, binding to the receptor may also induce allostery, leading to the dissociation of the dimer into active monomers, increasing the concentration of active monomers [37].

Rigid CXC versus flexible CC homodimers. Rigid homodimers may activate receptors with limited adaptability, which may lead to precise but less diverse signaling outcomes [38]. This rigidity may promote a focused or linear signaling cascade, as both receptor-binding sites are engaged in a fixed conformation. The lack of malleability may restrict the ability of rigid homodimers to bind to receptors that are spaced farther apart or in different orientations, potentially limiting their interactions with multiple receptors (Figure 4). The rigid homodimers of CXC ligands possess a fixed, well-defined interface between the two monomers, restricting conformational flexibility. The fixed distances between their binding sites necessitate specific spatial arrangements of receptors for optimal interaction, which can lead to increased specificity in receptor engagement. The rigid structure may promote simultaneous binding to two receptor monomers on the opposite cell in proximity. In contrast, flexible homodimers of CC ligands feature interfaces between the two monomers that allow for movement, enabling adaptability in receptor binding. This flexibility potentially permits the two binding sites to adjust and engage with receptors that may not be perfectly aligned, facilitating interactions with receptors on the same cell or different cells (Figure 4), even if they are spaced irregularly. The flexible structure can accommodate varying receptor conformations and types, including potential heterodimer formation, which enhances receptor cross-linking and oligomerization. Thus, a flexible ligand dimer can lead to a more robust and sustained signaling response. CC dimers may cross-link receptors on separate cells, promoting coordinated signaling among neighboring cells.

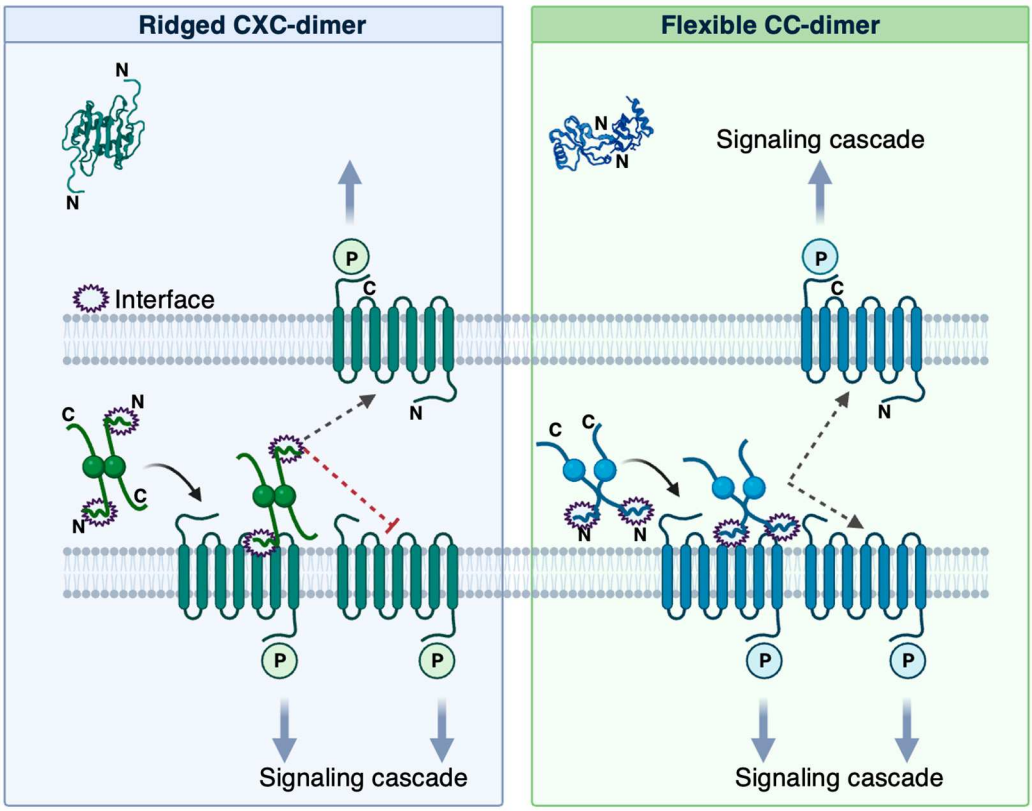

Figure 4. An illustration of ligand–receptor interactions. The rigid CXC dimer can exert a receptor cross-linking mechanism, i.e., the activation of two receptors on opposite cells. This can also occur for the more flexible CC dimers. Additionally, CC dimers can activate two receptors on the same cell. The arrows indicate the activation of chemokine phosphorylation (P) signaling pathways inside the cell.

4. Conclusions

Understanding protein dimers, their binding interfaces, and affinities is fundamental for elucidating their roles in cellular functions, elucidating disease mechanisms, and

advancing therapeutic and biotechnological applications. In this study, we investigated the binding affinities of six chemokine ligands, which range from 10 to 14 kcal/mol, to clarify their roles in receptor activation and biological signaling. The free energy for folding varies from 2 to 8 kcal/mol. Despite their low sequence identity, chemokine ligands display high structural similarity, creating a complex and adaptable system with approximately 24,000 possible ligand–receptor combinations that modulate the activity of 18 chemokine receptors if all 50 ligands can bind to all receptors through various oligomeric states. Our results reveal that the biophysical properties and calculated binding stability underscore the functional diversity of these proteins, despite their nearly identical three-dimensional structures in monomeric forms. We attribute these diverse biophysical characteristics to the sequence diversity among the ligands. This suggests that the malleability of the binding interface plays an important role in receptor interactions. Future directions of this research could involve exploring how the binding interface controls the dynamics of the ligands and potential downstream biological responses, further enhancing our understanding of chemokine signaling in health and disease.

Supplementary Materials: The following supporting information can be downloaded at: https://www.mdpi.com/article/10.3390/biophysica4040037/s1, Figure S1: The Mass spectrometry spectrum of (A) CCL2, (B) CCL8, and (C) CCL11 from MALDI-MS. The mass spectrometry experiments were conducted at Scripps Center for Metabolomics and Mass Spectrometry. Figure S2: Thermal melt of chemokine ligands. The data was collected on a v100 Chirascan utilizing the Pro-Data software (Applied Photophysics). (A) The raw data was normalized and plotted against temperature for CXC-ligands at a wavelength of 200 nm, 204 nm, and 207 nm for CXCL1, CXCL5, and CXCL8 respectively. Aggregation occurs after 80 °C for all three proteins. Furthermore, CXCL8 is not fully unfolded even at 90 °C where it exhibits residual secondary structure even at high temperatures. (B) The raw data was normalized and plotted against temperature for CC-ligands at a wavelength of 215, 230, and 230 nm for CCL2, CCL8, and CCL11 respectively. Figure S3: Predicted CCL11 dimer. The dimer structure is predicted with AlphaFold2 [39] and overlayed with the crystal structure of the monomer of CCL11 (PDB ID: 1EOT). Figure S4: (A) Sequence evolution. Sequence alignment using Clustal omega [40]. The fully conserved residues are highlighted with a * and boxed in red, C11, C12, C36, C52 and P55. The strongly conserved residues are highlighted with an : and boxed in blue. (B) The strongly conserved amino acids positioned at the core is highlighted (dark blue) in the structure of CCL8 and the non-conserved core residues are highlighted (light blue).

Author Contributions: Conceptualization, E.H., D.B. and J.P.; Methodology, E.H., D.B., Y.A.-H. and E.S.G.; Validation, E.S.G.; Formal analysis, E.H., D.B., Y.A.-H., J.P., J.M.P. and E.S.G.; Investigation, E.H., D.B., Y.A.-H., J.P. and E.S.G.; Data curation, E.H., D.B., Y.A.-H. and J.M.P.; Writing—original draft, E.H.; Writing—review & editing, E.H., D.B., Y.A.-H. and J.P.; Supervision, E.H. and E.S.G.; Project administration, E.H. and E.S.G.; Funding acquisition, E.H., Y.A.-H. and E.S.G. All authors have read and agreed to the published version of the manuscript.

Funding: The research reported by the Haglund group is supported by the National Science Foundation award number CHE2145906. Almeida and Sánchez García were supported by the CRC 1430 award number 424228829 and by the CRC 1279.

Data Availability Statement: All data is available in the manuscript and no deposits have been done elsewhere.

Conflicts of Interest: The authors declare no conflict of interest.

References

1. Sokol, C.L.; Luster, A.D. The chemokine system in innate immunity. *Cold Spring Harb. Perspect. Biol.* **2015**, *7*, a016303. [CrossRef] [PubMed]
2. Laub, M.T.; Goulian, M. Specificity in two-component signal transduction pathways. *Annu. Rev. Genet.* **2007**, *41*, 121–145. [CrossRef] [PubMed]
3. Hughes, C.E.; Nibbs, R.J.B. A guide to chemokines and their receptors. *FEBS J.* **2018**, *285*, 2944–2971. [CrossRef] [PubMed]
4. Mellado, M.; Rodriguez-Frade, J.M.; Vila-Coro, A.J.; Fernandez, S.; Martin de Ana, A.; Jones, D.R.; Toran, J.L.; Martinez, A.C. Chemokine receptor homo- or heterodimerization activates distinct signaling pathways. *EMBO J.* **2001**, *20*, 2497–2507. [CrossRef]
5. Miller, M.C.; Mayo, K.H. Chemokines from a Structural Perspective. *Int. J. Mol. Sci.* **2017**, *18*, 2088. [CrossRef]

6. Paavola, C.D.; Hemmerich, S.; Grunberger, D.; Polsky, I.; Bloom, A.; Freedman, R.; Mulkins, M.; Bhakta, S.; McCarley, D.; Wiesent, L.; et al. Monomeric monocyte chemoattractant protein-1 (MCP-1) binds and activates the MCP-1 receptor CCR2B. *J. Biol. Chem.* **1998**, *273*, 33157–33165. [CrossRef]
7. Wedemeyer, M.J.; Mahn, S.A.; Getschman, A.E.; Crawford, K.S.; Peterson, F.C.; Marchese, A.; McCorvy, J.D.; Volkman, B.F. The chemokine X-factor: Structure-function analysis of the CXC motif at CXCR4 and ACKR3. *J. Biol. Chem.* **2020**, *295*, 13927–13939. [CrossRef]
8. Wang, X.; Sharp, J.S.; Handel, T.M.; Prestegard, J.H. Chemokine oligomerization in cell signaling and migration. *Prog. Mol. Biol. Transl. Sci.* **2013**, *117*, 531–578. [CrossRef]
9. Monneau, Y.; Arenzana-Seisdedos, F.; Lortat-Jacob, H. The sweet spot: How GAGs help chemokines guide migrating cells. *J. Leukoc. Biol.* **2016**, *99*, 935–953. [CrossRef]
10. Gunasekaran, K.; Nussinov, R. How different are structurally flexible and rigid binding sites? Sequence and structural features discriminating proteins that do and do not undergo conformational change upon ligand binding. *J. Mol. Biol.* **2007**, *365*, 257–273. [CrossRef]
11. Gunasekaran, K.; Ma, B.; Nussinov, R. Is allostery an intrinsic property of all dynamic proteins? *Proteins* **2004**, *57*, 433–443. [CrossRef] [PubMed]
12. Arimont, M.; Sun, S.L.; Leurs, R.; Smit, M.; de Esch, I.J.P.; de Graaf, C. Structural Analysis of Chemokine Receptor-Ligand Interactions. *J. Med. Chem.* **2017**, *60*, 4735–4779. [CrossRef] [PubMed]
13. Penfield, J.; Zhang, L. Interaction and dynamics of chemokine receptor CXCR4 binding with CXCL12 and hBD-3. *Commun. Chem.* **2024**, *7*, 205. [CrossRef] [PubMed]
14. Garton, M.; MacKinnon, S.S.; Malevanets, A.; Wodak, S.J. Interplay of self-association and conformational flexibility in regulating protein function. *Philos. Trans. R. Soc. Lond. B Biol. Sci.* **2018**, *373*, 20170190. [CrossRef] [PubMed]
15. Martin, P.; Kurth, E.A.; Budean, D.; Momplaisir, N.; Qu, E.; Simien, J.M.; Orellana, G.E.; Brautigam, C.A.; Smrcka, A.V.; Haglund, E. Biophysical characterization of the CXC chemokine receptor 2 ligands. *PLoS ONE* **2024**, *19*, e0298418. [CrossRef]
16. Bittrich, S.; Segura, J.; Duarte, J.M.; Burley, S.K.; Rose, Y. RCSB protein Data Bank: Exploring protein 3D similarities via comprehensive structural alignments. *Bioinformatics* **2024**, *40*, btae370. [CrossRef]
17. Harder, M.E.; Deinzer, M.L.; Leid, M.E.; Schimerlik, M.I. Global analysis of three-state protein unfolding data. *Protein Sci.* **2004**, *13*, 2207–2222. [CrossRef]
18. Ge, B.; Jiang, X.; Chen, Y.; Sun, T.; Yang, Q.; Huang, F. Kinetic and thermodynamic studies reveal chemokine homologues CC11 and CC24 with an almost identical tertiary structure have different folding pathways. *BMC Biophys.* **2017**, *10*, 7. [CrossRef]
19. Evans, R.; O'Neill, M.; Pritzel, A.; Antropova, N.; Senior, A.; Green, T.; Žídek, A.; Bates, R.; Blackwell, S.; Yim, J.; et al. Protein complex prediction with AlphaFold-Multimer. *BioRxiv* **2022**. [CrossRef]
20. Lubkowski, J.; Bujacz, G.; Boque, L.; Domaille, P.J.; Handel, T.M.; Wlodawer, A. The structure of MCP-1 in two crystal forms provides a rare example of variable quaternary interactions. *Nat. Struct. Biol.* **1997**, *4*, 64–69. [CrossRef]
21. Bhusal, R.P.; Aryal, P.; Devkota, S.R.; Pokhrel, R.; Gunzburg, M.J.; Foster, S.R.; Lim, H.D.; Payne, R.J.; Wilce, M.C.J.; Stone, M.J. Structure-guided engineering of tick evasins for targeting chemokines in inflammatory diseases. *Proc. Natl. Acad. Sci. USA* **2022**, *119*, e2122105119. [CrossRef] [PubMed]
22. Fairbrother, W.J.; Reilly, D.; Colby, T.J.; Hesselgesser, J.; Horuk, R. The solution structure of melanoma growth stimulating activity. *J. Mol. Biol.* **1994**, *242*, 252–270. [CrossRef] [PubMed]
23. Sepuru, K.M.; Poluri, K.M.; Rajarathnam, K. Solution structure of CXCL5--a novel chemokine and adipokine implicated in inflammation and obesity. *PLoS ONE* **2014**, *9*, e93228. [CrossRef] [PubMed]
24. Clore, G.M.; Appella, E.; Yamada, M.; Matsushima, K.; Gronenborn, A.M. Three-dimensional structure of interleukin 8 in solution. *Biochemistry* **1990**, *29*, 1689–1696. [CrossRef] [PubMed]
25. Romero-Molina, S.; Ruiz-Blanco, Y.B.; Mieres-Perez, J.; Harms, M.; Münch, J.; Ehrmann, M.; Sanchez-Garcia, E. PPI-Affinity: A Web Tool for the Prediction and Optimization of Protein–Peptide and Protein–Protein Binding Affinity. *J. Proteome Res.* **2022**, *21*, 1829–1841. [CrossRef]
26. Gangavarapu, P.; Rajagopalan, L.; Kolli, D.; Guerrero-Plata, A.; Garofalo, R.P.; Rajarathnam, K. The monomer-dimer equilibrium and glycosaminoglycan interactions of chemokine CXCL8 regulate tissue-specific neutrophil recruitment. *J. Leukoc. Biol.* **2012**, *91*, 259–265. [CrossRef]
27. Herring, C.A.; Singer, C.M.; Ermakova, E.A.; Khairutdinov, B.I.; Zuev, Y.F.; Jacobs, D.J.; Nesmelova, I.V. Dynamics and thermodynamic properties of CXCL7 chemokine. *Proteins* **2015**, *83*, 1987–2007. [CrossRef]
28. Rumfeldt, J.A.; Galvagnion, C.; Vassall, K.A.; Meiering, E.M. Conformational stability and folding mechanisms of dimeric proteins. *Prog. Biophys. Mol. Biol.* **2008**, *98*, 61–84. [CrossRef]
29. Crump, M.P.; Rajarathnam, K.; Kim, K.S.; Clark-Lewis, I.; Sykes, B.D. Solution structure of eotaxin, a chemokine that selectively recruits eosinophils in allergic inflammation. *J. Biol. Chem.* **1998**, *273*, 22471–22479. [CrossRef]
30. Kleist, A.B.; Getschman, A.E.; Ziarek, J.J.; Nevins, A.M.; Gauthier, P.A.; Chevigne, A.; Szpakowska, M.; Volkman, B.F. New paradigms in chemokine receptor signal transduction: Moving beyond the two-site model. *Biochem. Pharmacol.* **2016**, *114*, 53–68. [CrossRef]
31. Allen, S.J.; Crown, S.E.; Handel, T.M. Chemokine: Receptor structure, interactions, and antagonism. *Annu. Rev. Immunol.* **2007**, *25*, 787–820. [CrossRef] [PubMed]

32. Mellado, M.; Vila-Coro, A.J.; Martinez, C.; Rodriguez-Frade, J.M. Receptor dimerization: A key step in chemokine signaling. *Cell. Mol. Biol. (Noisy-le-grand)* **2001**, *47*, 575–582. [PubMed]
33. Liu, K.; Wu, L.; Yuan, S.; Wu, M.; Xu, Y.; Sun, Q.; Li, S.; Zhao, S.; Hue, T.; Liu, Z. Structural basis of CXC chemokine receptor 2 activation and signaling. *Nature* **2020**, *585*, 135–140. [CrossRef] [PubMed]
34. Dyer, D.P. Understanding the mechanisms that facilitate specificity, not redundancy, of chemokine-mediated leukocyte recruitment. *Immunology* **2020**, *160*, 336–344. [CrossRef]
35. Stephens, B.; Handel, T.M. Chemokine receptor oligomerization and allostery. *Prog. Mol. Biol. Transl. Sci.* **2013**, *115*, 375–420. [CrossRef]
36. Handl, H.L.; Vagner, J.; Han, H.; Mash, E.; Hruby, V.J.; Gillies, R.J. Hitting multiple targets with multimeric ligands. *Expert. Opin. Ther. Targets* **2004**, *8*, 565–586. [CrossRef]
37. Fernando, H.; Chin, C.; Rosgen, J.; Rajarathnam, K. Dimer dissociation is essential for interleukin-8 (IL-8) binding to CXCR1 receptor. *J. Biol. Chem.* **2004**, *279*, 36175–36178. [CrossRef]
38. Romantini, N.; Alam, S.; Dobitz, S.; Spillmann, M.; De Foresta, M.; Schibli, R.; Schertler, G.F.X.; Wennemers, H.; Deupi, X.; Behe, M.; et al. Exploring the signaling space of a GPCR using bivalent ligands with a rigid oligoproline backbone. *Proc. Natl. Acad. Sci. USA* **2021**, *118*, e2108776118. [CrossRef]
39. Jumper, J.; Evans, R.; Pritzel, A.; Green, T.; Figurnov, M.; Ronneberger, O.; Tunyasuvunakool, K.; Bates, R.; Žídek, A.; Potapenko, A.; et al. Highly accurate protein structure prediction with AlphaFold. *Nature* **2021**, *596*, 583–589. [CrossRef]
40. Sievers, F.; Wilm, A.; Dineen, D.; Gibson, T.J.; Karplus, K.; Li, W.; Lopez, R.; McWilliam, H.; Remmert, M.; Söding, J.; et al. Fast, scalable generation of high-quality protein multiple sequence alignments using Clustal Omega. *Mol. Syst. Biol.* **2011**, *7*, 539. [CrossRef]